Endocrinology. First published ahead of print August 24, 2006 as doi:10.1210/en.2006-0503

Insulin-like peptide 6 (Insl6): Characterization of secretory status and post-translational modifications

Chunxia Lu[*], William H. Walker[‡], Jinhong Sun[*], Ora A. Weisz[‡§], Robert B. Gibbs[Φ], Selma F. Witchel[Ψ], Mark A. Sperling[Ψ], Ram K. Menon[*]

[*]Department of Pediatrics, University of Michigan, Ann Arbor, MI 48109, USA; Departments of [‡]Cell Biology and Physiology, [Ψ]Pediatrics, [§]Medicine, University of Pittsburgh School of Medicine, Pittsburgh 15213, USA, and [Φ]Department of Pharmaceutical Sciences, University of Pittsburgh School of Pharmacy, Pittsburgh 15260, USA

Abbreviated title: testis insulin-like peptide

Key words: germ cell, secretion, furin, ubiquination, glycosylation.

* Correspondence

Ram K. Menon, M.D.
University of Michigan Medical School
1205 MPB Box 0718
1500 E Medical Center Drive
Ann Arbor, MI 48109-0718

E-Mail: rammenon@umich.edu

DISCLOSURE STATEMENT - The authors have nothing to disclose.

Abstract

Insulin-like peptide 6 (Insl6) is a member of the insulin/relaxin superfamily with unknown biological function(s). In the current report, we establish that meiotic and post-meiotic germ cells of the testis are the principal sites of expression of Insl6. Analysis of stably or transiently transfected cells revealed that Insl6 is a secreted protein localized to the endoplasmic reticulum and Golgi. Secretion could be detected in both CHO and GC2 germ cells and was sensitive to brefeldin A treatment. In cell lysates, the predominant Insl6 band was approximately 28 kDa in size. In contrast, the predominant Insl6 species in the supernatant was 8 kDa in size, suggesting post-translational processing of the precursor protein. Ectopically expressed Insl6 is processed and secreted in furin deficient LoVo cells and in CHO cells treated with a furin inhibitor, although the size-profile of the secreted protein is altered suggesting that Insl6 is a substrate for furin action. Furthermore, mutation of a putative furin cleavage site in the Insl6 peptide resulted in aberrant processing of the Insl6 peptide. Additional investigations of the structure of Insl6 protein provided evidence for post-translational modifications of Insl6 including the presence of disulfide bonds, glycosylation, and ubiquitination. On the basis of the demonstrated secretory status of Insl6, we speculate that the physical proximity of the germ cell to the Sertoli cell renders the Sertoli cell a likely candidate for Insl6 action.

Introduction

The insulin / IGF / relaxin family is an ancient family of functionally diverse proteins. Insulin or insulin-like proteins have been described in unicellular eukaryotes, primitive species such as insects, tunicates, annelids, and molluscans (1-6). Despite functional divergence within the family, all proteins of the insulin family exhibit a high degree of structural conservation. The primary peptide sequence of each member of the family is characterized by three domains comprised of an amino terminal B peptide (or chain) joined to a carboxyl A peptide by an intervening C peptide (B-C-A) (7). Between the different hormones of the family and between species for a specific hormone, the B and A chain peptides are relatively invariant and exhibit a pattern of distinct and highly conserved cysteine motifs. These cysteine motifs characterize the family; specifically the motif present in the A peptide has been termed the insulin signature. Many members of the insulin family of hormones are synthesized as preprohormones with the primary peptide undergoing post-translational modification to generate a disulfide bond-linked heterodimer of the B and A peptides that functions as the active hormone.

At the beginning of the past decade, the insulin family was comprised of four members in mammals; insulin, the insulin-like growth factors (IGF I and IGF II) and relaxin. Over the past decade additional members of the family termed INSL3 (8, 9), INSL4 (10, 11), INSL5 (12, 13), INSL6 (13-15), and INSL7 (16) have been identified. The precise biological role(s) of many of these new proteins, including Insl6 remains to be determined. Although previous studies had established that the testis is the site of maximum expression of Insl6, there is discordance amongst published studies as to the cell-type in the testis in which Insl6 is expressed. Hsu localized expression to Leydig cells (13), while Lok *et al.* concluded that Insl6

is expressed in pachytene spermatocytes and round spermatids but not in Leydig cells (15). At present information regarding the secretory status, post translational modifications and processing of Insl6 protein is lacking. The aims of this study were to determine the identity of the cell-type expressing Insl6 in the testis, to investigate the sub-cellular localization and secretory status of Insl6, and to identify and characterize potential post-translational modifications and processing of this protein.

Materials and Methods

Cell culture: The culture media used for tissue culture experiments were obtained from Life Technologies, Inc. unless otherwise stated. Flp-In CHO cells (Invitrogen, Inc.) and mInsl6-CHO cells were grown at 37^0C in F12 medium supplemented with 10% fetal bovine serum (FBS). Germ cell (GC2), CRE8 cells, HEK293 and LoVo cells were grown in DMEM (4.5g/L glucose) with 10% FBS.

Generation and characterization of anti-Insl6 antibody: Employing the services of a commercial vendor (Biosource, Inc.), anti-mouse Insl6 sera were raised in the rabbit against keyhole hemocyanin conjugated peptides termed EE and YV representing amino acid residues 56 to 71 and 134 to 150 respectively; both peptides overlap with the putative C peptide (14). The antisera were affinity purified against the homologous peptide using standard techniques. The specificity of the antibodies was verified by demonstrating that the homologous peptide (200 molar excess) was able to block the detection of the Insl6 protein by Western blot analysis whereas insulin failed to exhibit such competition (data not shown). In certain experiments, an anti-A chain mInsl6 antibody from Phoenix Pharmaceuticals, Inc was used.

Animals: Eight week old male mice (C57BL) (Hilltop, PA) and testicular tissues from WBB6F1/J-Kit^w/Kit^{W-v} or WB/ReJ Kit^w/+ mice (Jackson Laboratory) were purchased. Female Sprague-Dawley rats carrying pups at 19 days gestation were exposed to a single dose of whole-body X-ray-irradiation equivalent to a dose of 200 rads using a ^{137}Cs source. Age matched, non-irradiated females were employed as controls. The pups were born spontaneously on day 22 and sacrificed nine weeks after birth. All experiments were carried

in accordance with protocols approved by the Institutional Animal Care and Use Committees at the Children's Hospital of Pittsburgh, the University of Pittsburgh, or the University of Michigan.

Tissue collection: Euthanized animals were perfused with ice-cold saline followed by 4% paraformaldehyde in 50 mM sodium acetate (pH 6.5) and then with 4% paraformaldehyde in 50 mM Tris-HCl (pH 9.0). Testes were removed and postfixed in 4% paraformaldehyde in phosphate buffer (pH 7.2) at 4°C overnight. Testes were sequentially immersed at 4°C for 24 h periods in phosphate buffer (for paraffin embedding) or in 15% sucrose in phosphate buffer followed by 30% sucrose in phosphate buffer (for collecting frozen sections). Paraffin sections (10 µm), and frozen sections (20 µm) were cut and mounted onto Super Frost Plus glass slides (Fisher Scientific, Inc.). Paraffin sections were stored at room temperature and frozen sections were stored at -20°C prior to staining.

Staining: Paraffin sections were first deparaffinized with xylene and rehydrated with 50 mM PBS. Frozen sections were thawed in a dessicator at room temperature and then hydrated with 50 mM PBS. All sections were treated with 0.3 % H_2O_2 in PBS for 15 min to inactivate endogenous peroxidase activity. Tissues were then rinsed with PBS and primary antibody was applied at a dilution of 1:5000 or 1:10000 in PBS containing 0.05% Triton X-100 and 5% normal goat serum. Control sections were either not exposed to the primary antibody or were treated with the primary antibody plus blocking peptide (10 µg/ml). Sections were incubated for 3 days at 4°C. Sections were then rinsed with PBS and treated with biotinylated goat-anti-rabbit IgG (3.0 µg/ml, Vector Laboratories, Inc.) for 3 h at ambient temperature. Sections

were then rinsed with PBS. Antibody binding was visualized using the avidin-biotin-HRP Elite system (Vector Labs, Inc.). The avidin-biotin-HRP reagent was utilized at a concentration of 5µl/ml each of reagent A and B in 50 mM PBS and incubated for 3 h at ambient temperature. Sections were reacted in a solution containing 3-3' diaminobenzidine (0.5 mg/ml, Sigma, Inc.), 0.01% H_2O_2, and 0.03% NiCl in 50 mM Tris-HCl (pH 7.6) for 10 min. After antibody staining, sections were rinsed with PBS, some were counterstained with Mayers hematoxylin solution (Sigma, Inc.), dehydrated with ethanol, cleared with xylenes, and cover slipped with DePeX (Gurr, Inc.). For the tissues that were stained with Cy-3, the biotinylated secondary and avidin-biotin-HRP steps were omitted. Sections were incubated with Cy-3 labeled goat-anti-rabbit IgG (7.5 mg/ml, Jackson Laboratories) in 50 mM PBS+ .05% Triton for 1 h at room temperature. The sections were rinsed with 50 mM PBS, counterstained with Sytox Green (1:5000) for 5 min, and rinsed again with PBS. The sections were then rinsed briefly with water and overlaid with coverslips using Gel/Mount (Biomedia Corp.) aqueous mounting media.

Plasmid construction and generation of Insl6 expressing stable cell line: The mInsl6-TOPO II and hInsl6-TOPO II constructs were generated by cloning murine or human Insl6 cDNA, respectively into the TOPOII vector (Invitrogen, Inc.). The plasmids encoding mInsl6 or hInsl6 fused at the C-terminus to the myc-His tag was generated by subcloning Insl6 cDNA into the eukaryotic expression vector, pcDNA3.1(+) myc-his (Invitrogen, Inc.). CHO cells stably expressing mInsl6 (mInsl6-CHO) was generated using the Flp-In system (Invitrogen, Inc.) as per the manufacturer's protocol. Briefly, Insl6 tagged at the C-terminus with the myc-his epitope was cloned into Flp-In expression vector, pcDNA5/FRT. Flp-In CHO host cells

were co-transfected with Insl6-myc-his pcDNA5/FRT and the Flp recombinase expression vector pOG44. Isogenic expression cell lines were isolated using hygromycin selection.

Recombinant adenovirus expressing murine Insl6. Myc-His epitope tagged mouse Insl6 gene was subcloned into at the Sma I site of the pAdlox plasmid (Somatix Therapy Co.) (17). Three micrograms each of the recombinant pAdlox plasmid and the ψ5 helper virus was transfected into Cre8 cells using Lipofectomine (Invitrogen). The culture medium was replaced every two days and the cells along with the media harvested in 7-8 days when the majority of the cells had rounded or detached. Cre8 cells were re-infected twice with the cell lysate to purify and amplify the recombinant virus (Ad-mInsl6). Virus titer was determined by plaque assay in HEK293 cells.

Production of Recombinant mInsl6 with mutation in putative furin cleavage site: The putative furin cleavage motif (RKRR) in mInsl6 peptide located between amino acids 162 - 165 was mutated (to AAAA) using the QuickChange Site-Directed Mutagenesis Kit (Stratagene, La Jolla, CA) according to the manufacturer's instructions.

Immunofluorescence staining: mInsl6-CHO stable cells or Ad-mInsl6 infected GC2 cells were fixed with 4% paraformaldehyde and permeablized with 0.1% Triton-X 100. Double staining with rabbit or mouse anti-myc (1:100 dilution) and rabbit anti-Grp78 (1:100) or mouse GM130 (1:100) antibody was visualized by FITC-labeled anti-mouse IgG and Rhodamine-labeled anti-rabbit IgG. Cells were observed using a confocal microscope (Olympus FluoView 500) or a Nikon TE200 Eclipse fluorescence microscope. In certain

experiments the cells were exposed to nocodazole (20 μM for 60 min on ice) prior to fixation and immunofluorescence staining.

Transient transfection: 0.4×10^6 CHO cells were plated on 35-mm plates 24 h prior to transfection. 3 μg of plasmid DNA was transfected per plate using the Lipofectamine method (Life Technologies, Inc.). After 6 h of incubation, the DNA-Lipofectamine mixture was removed and then supplemented with medium for 48 h prior to harvest for Western blot analysis.

Infection of GC2 cells with Ad-mInsl6. GC2 cells were infected with Ad-mInsl6 at 30 pfu/cells. In indicated experiments infected cells or supernatant from the infected cells were harvested after 48 hours following exposure of the cells to either brefeldin (BFA) or vehicle.

Deglycosylation assay: Protein extracts (lysed in RIPA buffer containing 50 mM Tris-HCl pH 7.5, 150 mM NaCl, 2mM EGTA and 0.1% Triton X-100) from CHO cells transiently transfected with Insl6 expressing plasmid or GC2 cells infected with Ad-mInsl6 were treated with N-glycosidase F (PNGase F) or Endoglycosidase H (New England Biolabs) according to the manufacturer's protocol. For PNGase F treatment, 10 μl aliquot of protein was mixed with 1 μl 10X denaturation buffer and boiled for 10 min. The denatured protein mixture was mixed with 1 μl 10X reaction buffer, 1 μl of 10% NP 40 and 1 μl of PNGase F. The reaction was carried out at 37^0C for 1-4 hours. For Endo H treatment, 30 μg aliquots of protein extracts were denatured with 1X glycoprotein denaturing buffer at 100°C for 10 minutes and then

treated with 500 units Endo H in the presence of 1X of reaction buffer (50 mM sodium citrate, pH 5.5) for 1 hour at 37°C. The reactions were stopped by boiling in SDS-sample buffer at 100^0C for 5 min and analyzed by SDS-PAGE.

Western blot analysis: CHO or LoVo cells transiently transfected with Insl6 plasmid construct or CHO cells stably expressing Insl6 were harvested at indicated time points. GC2 cells infected with Ad-mInsl6 were harvested after 48h of infection. Brefeldin A (BFA, Sigma) treatment was performed by exposing cells to BFA (1 to 50 ug/ml) for the indicated time periods. Cells were washed twice with cold PBS, lysed in RIPA buffer (50 mM Tris-HCl pH 7.5, 150 mM NaCl, 2mM EGTA and 0.1% Triton X-100) supplemented with a protease inhibitor cocktail (Roche), supernatant precipitated with 15% TCA, and the protein pellet resuspended in 1% SDS. Equal amounts protein were size-fractionated via SDS-PAGE and subjected to Western blot analysis as previously described (18) . The primary antibodies used in these analyses was anti-myc (9E10, Santa Cruz, Inc.) routinely used at a dilution of 1:500. All results are representative for three or four independent experiments.

LDH activity assay: Cytotoxicity was determined using a cytoxicity detection kit (Roche). Briefly, 100 µl supernatant aliquot was mixed with 100 µl reaction mixture and incubated for 20 min at room temperature. Low and high controls for the assay were established by assaying the cell culture medium and the supernatant of Triton X-100 treated cells respectively. The cytotoxicity index (CI) was determined by the equation: CI = (sample - low control) ÷ (high control-low control) × 100.

In vitro transcription and translation: Transcription and translation coupled reticulocyte lysate and wheat germ extract systems were purchased from Promega, Inc. The reactions were initiated by mixing 3µg Insl6-TOPO II plasmid DNA with 50µl reticulocyte lysate or wheat germ extract reaction mixtures in the presence of [^{35}S] cysteine (ICN) and T7 polymerase. Following incubation at 30^{0}C for 90 min, the products were size-fractionated via electrophoresis through a 14% SDS-PAGE gel. In some reactions His-ubiquitin (Sigma, Inc.) was added at the initiation of the reaction (19). Where indicated the intensity of the specific bands was quantitated by densitometry (Bio-Rad, Inc.).

RNA extraction: Total RNA was extracted from testes either via a guanidine isothiocyanate-based technique followed by cesium chloride gradient purification or by using TRI-Reagent (Molecular Research Center, Inc.) (20).

Real-Time RT-PCR assay: Real-time quantitative RT-PCR using the ABI Prism 7700 Sequence Detection System (PE Biosystems; Foster City, CA) was carried out using established protocols (21) . The primers (synthesized by Life Technologies) and TaqMan probes (synthesized by PE Biosystems) for the quantitation of the Insl6 and LH receptor transcripts were designed using the primer design software Primer Express (PE Biosystems; Foster City, CA) (Table 1). The primers and TaqMan probe for 18S rRNA were purchased from a commercial vendor (PE Biosystems; Foster City, CA). The 18S probe was labeled with reporter fluorescent dye VIC and the Insl6 and LH receptor probes with the reporter dye FAM. The relative efficiencies of the Insl6 and LH receptor primers/probe sets and the 18S primer/probe pair were tested by subjecting serial dilutions of a single RNA sample from each

of the tissues analyzed to real-time RT-PCR analysis. The plot of log input versus ΔC_T was <0.1, which satisfies the previously established criterion for equivalence of efficiency of amplification (22) . After confirming that the efficiency of amplification of the gene of interest (e.g. Insl6) and 18S transcripts were approximately equal, the amount of the transcripts for the specific gene relative to the 18S transcript was determined by using the comparative C_T (separate tube) method (22). Briefly, 5 ng aliquots of total RNA were analyzed using the One-Tube RT-PCR protocol (PE Biosystems). Following reverse transcription at 48^0C for 30 min, the samples were subjected to PCR analysis using the following cycling parameters: 95^0C x 10 min; 95^0Cx 15 sec $\rightarrow$ 60^0C x 1 min for 40 cycles. Each sample was analyzed in triplicate in individual assays performed on two or more occasions.

Results

Cellular Localization of Insl6 in Mouse Testis

Two strategies were used to determine the cellular localization of Insl6 expression in the rodent testis.

Immunocytochemistry – For purposes of immunostaining with anti-Insl6 antibody we evaluated both paraffin and frozen testis sections. The staining observed under both conditions was similar with the exception that staining of the frozen sections tended to be denser. Using an anti-peptide antibody (EE) directed against an epitope of the Insl6 encompassing contiguous portions of the B and C chains of the Insl6 molecule, we observed staining of the germ cells of the testis. The germ cells stained with the Insl6 antibody were mid pachytene spermatocytes, secondary spermatocytes and round spermatids (Fig. 1A). Pre-incubation of the antibody with the homologous peptide abrogated the staining indicating that the observed staining was specific (Fig. 1B). Counter-staining with a nucleus-specific stain (Sytox green; Molecular Probes) indicated that in germ cells Insl6 was excluded from the nucleus and was localized to the cytoplasmic region (Fig. 1C). No specific staining of either Leydig or Sertoli cells was detected. Similar results (data not shown) were observed with an anti-peptide antibody (YV) directed against a second epitope of the murine Insl6 protein.

Effect of germ cell aplasia on Insl6 expression - Irradiation of the fetal testis results in preferential loss of germ cells in postnatal life. We exploited this model to investigate the cellular localization of Insl6 in the rat testis. Using a real-time quantitative RT-PCR technique we measured the steady-state abundance of Insl6 mRNA in the testis of 9 week old male rats that had been subjected to irradiation during fetal life. The expression of Insl6 in the testis of

the irradiated rats was 10-20% of age-matched non-irradiated controls (Fig. 2A). To validate the model for preferential loss of germ cells, we measured the levels of the Leydig cell-specific LH receptor mRNA in these samples. The abundance of the LH receptor mRNA in the testis of the rats exposed to radiation *in utero* was increased. This increase in the steady state abundance of LH receptor RNA reflects the relative enrichment of testicular tissue for Leydig cells following the radiation-induced loss of the germ cell which is the predominant cell type in the mature testes. Hence these results confirm the relative sparing of the Leydig cell in this model. Insl6 mRNA expression was also undetectable in the testis of mice with germ cell aplasia due to a mutation in the *kit* oncogene (WBB6F1/J-$Kit^{W}/Kit^{W\text{-}v}$) (Fig. 2B). Thus in the absence of germ cells, despite the presence of Leydig cells, Insl6 mRNA was essentially undetectable in the testis.

Expression of Insl6

Ontogeny of expression of Insl6 in mouse testis - Real-time RT-PCR assay was used to characterize the ontogenic profile of expression of Insl6 in mouse testis. Insl6 mRNA expression was detectable at low levels at embryonic day 14.5 & 17.5, and the level of expression remained low (0d & 7d postnatal) until postnatal day 20 when there was a 40-50 fold increase in Insl6 mRNA abundance with maximum levels attained by 40d and maintained up to 90d of age (Fig. 3A). Notably pachytene spermatocytes, identified in our studies as a major site of expression of Insl6, first appear in the mouse testis around postnatal day 20.

Expression of Insl6 in other mouse tissues - Real-time RT-PCR assay was used to characterize the quantitative profile of expression of Insl6 in various mouse tissues. Whereas

Insl6 mRNA expression was most abundant in the testis, Insl6 mRNA was also detected in intestine, thymus, kidney, uterus, ovary, spleen, breast, lung, and liver. However, the level of expression in these tissues was only 1-8% of that observed in the testis (Fig. 3B). Steady state abundance of Insl6 mRNA in GC2 cells, a murine germ cell line, was also only 1% of that measured in the intact mouse testis (data not shown).

Intracellular localization of Insl6 - The sub-cellular localization of Insl6 was investigated by co-localization studies of both CHO cells stably expressing either mInsl6 or hInsl6, and GC2 cells expressing adenoviral-mediated mInsl6. Staining with antibodies directed against Bip (Fig. 4A) and GM130 (Fig.4B) proteins as marker for the ER and the Golgi apparatus respectively revealed that in both CHO and GC2 cells, Insl6 protein co-localized to the perinuclear ER region and to the Golgi apparatus. Furthermore exposure of the cell to nocodazole, a reagent that disrupts microtubules and causes fragmentation of the Golgi apparatus, revealed that there was parallel redistribution of GM130 and Insl6 indicative of localization of Insl6 to the Golgi apparatus (Fig.4B).

Post-Translational Processing and Modifications of Insl6

At present, information about the biological role(s) of Insl6 is not available. As a first step towards identification of the putative biological role(s) of Insl6 we analyzed the Insl6 protein for post-translational processing and modifications.

Insl6 is a secreted protein - Based on the knowledge that canonical members of the insulin family are secreted proteins, the possibility of Insl6 being a secreted protein was tested by

analyzing the supernatant of CHO cells stably transfected with mInsl6 (mInsl6-CHO) and GC2 cells infected with adenovirus expressing mInsl6 (Ad-mInsl6). As shown in figure 5, mouse Insl6 protein could be detected in the supernatant of both cell types, supporting the hypothesis that Insl6 is a secreted protein. In contrast to the cell lysate where the predominant species was 28 kDa in size (top panel), in the cell culture supernatant a substantial fraction of the secreted Insl6 was 8 kDa in size (bottom panel). A similar size profile of Insl6 protein was also observed in CHO cells transiently transfected with mInsl6 (data not shown). These results suggest that the 8 kDa form represents a processed form of the precursor 28 kDa species of mInsl6.

To examine the possibility that Insl6 protein in supernatant was released from the lysis of dead cells, we investigated the effect of BFA, a yeast metabolite that blocks protein translocation from ER to Golgi, on Insl6 secretion in mInsl6-CHO (Fig. 6A) and Ad-mInsl6 infected GC2 cells (Fig. 6B). These results demonstrate that BFA inhibited the secretion of Insl6 (the 8 kDa band) into the cell culture supernatant (Fig. 6A- top panel and Fig. 6B). This dose-dependent effect of BFA in both CHO and GC2 cells, supports the conclusion that Insl6 is secreted into the medium and the presence of Insl6 in the cell culture supernatant is not the result of lysis of dead cells. Analysis of the whole cell lysates (Fig. 6A- bottom panel) verified that BFA did not inhibit the synthesis of the 28 kDa Insl6 precursor, supporting the conclusion that the observed BFA-dependent decrease in Insl6 in the cell culture supernatant was not the result of decreased synthesis of the Insl6. To obtain a quantitative measure of cell lysis, we assayed the cell culture medium from mInsl6-CHO for LDH activity (an index of cell death) and calculated the cytotoxicity index. These results indicate that there was no significant changes in the cytotoxicity index in the transfected cells (10-12%) as compared to

the untransfected cells (9-10%), further supporting the secretory status of Insl6 protein in these model systems. In contrast, adenoviral infection of GC2 cells resulted in a limited degree of cell death. In this context the 28 kDa band detected by Western blotting of the cell supernatant of GC2 expressing adenovirally expressed Insl6 (Fig 6B) possibly represents Insl6 precursor released from the lysis of the dead cells. This scenario would also be compatible with the observed insensitivity of the 28 kDa band to treatment with BFA (Fig 6B).

Insl6 is a target for processing by furin - *In silico* analysis of the primary structure of the mInsl6 amino acid sequence indicated the presence of a single furin recognition motif (RKRR) at aa 162 – 165. To investigate the role of furin in the post-translational processing of the Insl6 protein, furin deficient LoVo cells were transfected with wild type mInsl6 or a mutant mInsl6 peptide in which the putative furin preferred consensus sequence RKRR was mutated to AAAA (Fig.7). Whereas secretion of mInsl6 was intact in the LoVo cells, the size-pattern of the secreted proteins was altered in these cells. Thus in LoVo cells transfected with wild type mInsl6, a single protein band of approximately 8 kDa was detected in contrast to two bands of 8 and 6 kDa detected from mInsl6-CHO cells (Fig 7 - upper panel). Similar results were also obtained by treating mInsl6-CHO cells with the furin inhibitor Dec-RVKR-CMK (Fig 7 – lower panel). Complementation of LoVo cells via ectopic expression of furin reverted the secretion pattern of mInsl6 to that observed in CHO wild type cells with the appearance of the 8 and 6 kDa bands (Fig. 7- upper panel, lane 4). These results indicate that furin plays a role in the processing of the Insl6 prohormone. Furthermore, the molecular size of the secreted mutant mInsl6 increased to approximately 16 kDa in both CHO (Fig. 7- upper

panel, lane 2) and LoVo (Fig. 7- upper panel, lane 6) cells indicating that the RKRR sequence is the target for action of both furin and a non-furin PC and is essential for the complete processing of the Insl6 peptide.

Insl6 is linked by disulfide bonds - The primary structure of B and A peptides of mInsl6 reveal conserved cysteine motifs that are a hallmark of the insulin/relaxin protein superfamily. To investigate if these cysteine motifs result in the formation of intra/intermolecular disulfide bonds in mInsl6 protein, cell lysates (Fig. 8A; top panel) or supernatants (Fig. 8A; bottom panel) of mInsl6-CHO stable cells were size-fractionated through a 15% PAGE gel under either non-reducing or reducing conditions and then subjected to Western blot analysis. In cell lysates (Fig. 8A; top panel) mInsl6 migrated at a faster rate in the non-reducing (lane 1-2) as compared to reducing milieu (lanes 3-6). These results are compatible with the presence of intramolecular disulfide bonds in the precursor species. In contrast, in the cell culture supernatant (Fig. 8A, bottom panel) under non-reducing conditions (lane 2), the size of secreted mInsl6 was larger (14-16 kDa) compared to the size observed with reducing condition (8 kDa) (lanes 3-5). These findings can be explained by a model of mInsl6 characterized by the presence of intermolecular disulfide bonds linking B and A peptides; the 14-16 kDa species representing the B and A disulfide linked secreted Insl6 protein, and the 8 kDa species representing the epitope-tagged A peptide.

We next investigated whether the human Insl6 protein also exhibited a similar secondary/tertiary structure. In contrast to the murine peptide, there was no alteration in the electrophoretic mobility of the 10 kDa secreted human peptide in reducing vs non-reducing conditions (Fig. 8B). This observation, obtained in both CHO (Fig. 8B) and in LoVo cells

(data not shown), suggests the absence of disulfide bonds (and hence of the B peptide) in the secreted hInsl6 peptide. An alternate explanation is that the absence of the B peptide in the secreted hInsl6 protein is due to aberrant processing of hInsl6 and is an artifact of the cell culture models (CHO and LoVo cells) employed.

Differential N-linked glycosylation of murine and human Insl6 proteins - An *in silico* analysis of the primary structure of the human and murine Insl6 protein sequence using the NetNGly 1.0 (www.cbs.dtu.dk/services) software program predicted the presence of a single N-linked glycosylation site (at residue 49 in the human and residue 158 in the mouse). This prediction was tested by analyzing the effect of Peptide N-Glycosidase F (PNGase F), on the electrophoretic mobility of recombinant Insl6 proteins in cell lysate. The electrophoretic mobility of the murine prepro/pro-Insl6 protein in cell lysates was unaffected (Fig. 9A, bottom panel). In contrast, the electrophoretic mobility of the human prepro/pro-Insl6 peptide was increased by treatment of cell lysates with PNGase F suggesting that the human protein is modified by N-linked glycosylation (Fig. 9A, upper panel). However we were unable to confirm that the secreted hInsl6 peptide is also glycosylated. This is because the predicted glycosylation site on the hInsl6 peptide is located on the putative B peptide, and as detailed in the prior section we were unable to detect the presence of the B peptide in the secreted hInsl6 peptide. To exclude the possibility that CHO is not an appropriate model system to investigate the glycosylation status of Insl6, we subjected Insl6 ectopically expressed in GC2 to similar analysis. These results (Fig. 9B) verified the presence of N-linked glycosylation in human prepro- or pro-Insl6 and its absence in the murine protein. To further characterize the nature of the glycosylation of the human Insl6 precusor, we tested the effect of Endoglycosidase H

(Endo H), on recombinant human Insl6 protein. The human Insl6 protein was susceptible to Endo H treatment indicating the presence of immature high mannose residues (Fig. 9C). We confirmed the lack of effect of endoglycosidase F on mouse Insl6 by examining mouse testis extracts (Fig 9D, upper panel). To ascertain the specificity of the anti-Insl6 antibody used to detect endogenous Insl6 in mouse testes, we tested two anti-mInsl6 peptide antibodies, custom made EE antibody directed against the C chain (Fig 9D, top panel) and the commercially available anti-A chain antibody (Phoenix Pharmaceuticals, Fig 9D, bottom panel). Western blot analysis of intact testes and primary germ cell extracts with either of these antibodies revealed the presence of a 24 kDa doublet band compatible with prepro- or pro-Insl6 protein. In contrast a specific signal was not detected in liver extracts. In addition to the 24kDa doublet, bands that migrated at 15kDa and 30kDa were observed when testis extracts were blotted with the EE antibody. The identity of these bands is not clear at the present time. The 15kDa band could represent a B-C chain intermediate form of Insl6. The 30kDa band is possibly non-specific since this band was not observed in germ cell extracts blotted with the anti-A peptide antibody.

Insl6 is ubiquinated - To investigate whether Insl6 can be subjected to other post-translational modification such as ubiquination, recombinant mInsl6 protein was synthesized *in vitro* by coupled transcription and translation reaction using either rabbit reticulocyte lysate or wheat germ extract systems. In addition to the full-length protein, the mInsl6 protein produced with the reticulocyte lysate, but not the wheat germ lysate, exhibited bands of higher molecular mass (lane 2, Fig. 10A). These higher molecular mass bands were spaced at approximately 8 kDa intervals. A similar profile was observed with the recombinant human Insl6 protein (data

not shown). The spacing of the bands suggested the possibility that the Insl6 protein could be ubiquinated. To confirm this hypothesis, the coupled transcription and translation reaction in the reticulocyte lysate system was carried out in the presence of His-tagged ubiquitin (lane 3, Fig. 10A). The appearance of novel bands of higher molecular weights corresponding to the addition of the His epitope establishes that Insl6 is ubiquinated *in vitro* (19). The size of the higher molecular bands indicated that less than four molecules of ubiquitin were added to one Insl6 protein, indicating that Insl6 is predominantly subjected to mono- rather than poly-ubiquination. A characteristic feature of ubiquination is its dependence on ATP, which is required for conjugation of ubiquitin to the substrate and for degradation of the ubiquinated protein (19). To obtain further proof of Insl6 being ubiquinated, we tested the effect of depletion of ATP on the *in vitro* degradation of Insl6. Depletion of ATP from the reticulocyte lysate mixture by addition of 2-deoxyglucose and hexokinase resulted in an inhibition of degradation of Insl6 (Fig. 10B). This sensitivity of degradation of Insl6 to ATP concentration is consistent with the Insl6 protein being ubiquinated.

Ubiquinated proteins are targeted for degradation via the proteasome pathway and/or via lysosomal degradation. To determine whether degradation of Insl6 involves the proteasome machinery, CHO cell stable expressing mInsl6 were exposed to either clasto-Lactacystin β-lactone (a proteasome inhibitor) or DMSO (vehicle) and the amount of Insl6 protein quantified by Western blot analysis (Fig. 10C). These results revealed that treatment with clasto-Lactacystin resulted in increase in the steady levels of Insl6 in these cells suggesting that the degradation of Insl6 involves the proteasome pathway. To further explore this possibility, clasto-Lactacystin or DMSO was added into an *in vitro* translation system designed to translate the mInsl6 protein. As shown in Fig 10D, addition of clasto-Lactacystin

partially inhibited the degradation of the *in vitro* synthesized Insl6. Similar results were obtained via pulse chase experiments (Fig. 10E) wherein exposure of CHO cells stably expressing Insl6 to clasto-Lactacystin resulted in a modest prolongation of the half-life of Insl6 from 45 min to 80 min. The lack of total inhibition of Insl6 degradation following blockade of the proteasome pathway prompted an investigation of alternate routes for intracellular protein degradation. Thus exposure of Insl6 stably expressing CHO cells to the lysosome inhibitors chloroquin resulted in a more pronounced abrogation of degradation of Insl6 indicating the participation of the lysosomal pathway in Insl6 degradation (Fig. 10E).

Discussion

Insl6 is a recently identified member of the insulin/relaxin gene superfamily whose biological role is yet to be defined (13-15). The goal for the present study was to gain insights into the biological actions of Insl6. The main findings of the current study are that Insl6 is a secreted protein expressed in the germ cells of the testis, Insl6 undergoes post-translational modifications including prohormone processing, disulfide bond formation, N-linked glycosylation, and ubiquitination, and that Insl6 is a target for furin action.

Our results indicate that the site of maximal expression of Insl6 is the germ cell of the testis and that expression of Insl6 is restricted to the mid pachytene spermatocytes, secondary spermatocytes and round spermatids stages of germ cell maturation. Whereas a previous report (15) had also concluded, on the basis of *in situ* hybridization studies, that Insl6 was predominantly expressed in the germ cell of the testis, Hsu reached the disparate conclusion that Leydig cells are the exclusive site of expression of Insl6 (13). The reason(s) for the discrepancy between the results of the immunohistochemical experiments conducted by Hsu and those of the current study is not clear. Whereas our results do not exclude the possibility that the Leydig cell may also be a site of expression of Ins6, our results do establish unequivocally that the germ cell is the principal site of Insl6 expression in the adult testis. This conclusion is based on multiple lines of evidence including immunohistochemistry, expression profile of Insl6 mRNA in models of germ cell depletion, and ontogenic profile of mRNA expression in the testis.

Characterized members of the insulin/relaxin superfamily all are secreted proteins with signal peptides in their primary structure and intra- and inter-molecular cysteine-linked disulfide bonds in the mature protein. In the present study, we demonstrate that Insl6 is also a

secreted protein containing disulfide bonds with intracellular localization to the ER and Golgi. Secretion of Insl6 was confirmed in both CHO and GC2 cells. This secretion could be blocked by Brefeldin A (BFA) treatment suggesting that Insl6 is secreted through a classic secretory pathway. Ectopic expression of Insl6 in either CHO or GC2 cells resulted in two major bands. In cell lysates, the predominant Insl6 band was approximately 28 kDa in size. In contrast in the supernatant, the dominant band was a doublet of 6/8 kDa (putative A peptide) in size under-reducing conditions and 12/14 kDa (putative A+B peptide) under non-reducing conditions. Our results establish for the first time that Insl6, like other members of the insulin family, is processed from precursor (28 kDa) to mature protein (14kDa) and that the mature protein is linked by disulfide bonds. BFA treatment blocked the secretion of Insl6 in both CHO and GC2 cells, suggesting that the 8 kDa Insl6 peptide is processed and secreted, and does not result from non-specific degradation of dead cells.

Mouse prepro-Insl6 has 191 amino acids. Since this protein was fused with the myc-His tag, the total number of amino acids for the fused protein is 225 and the predicted size of this protein on SDS-PAGE is approximately 25 kD for prepro-mInsl6 and 22kD for pro-mInsl6. Our results indicate that the putative mouse pro-Insl6 migrated as a 28kD doublet, 11%-14% larger than expected. At the present time the reason(s) for the Insl6 precursor migrating as a doublet is not clear. We ruled out the possibility of incomplete reduction of disulfide bonds resulting in oxidized and reduced forms of the protein by treating the protein samples with the alkylating agent iodoacetamide prior to electrophoresis (data not shown). However this treatment failed to alter the doublet configuration of the mouse pro-Insl6 protein, indicating that the doublet configuration is not consequent to incomplete reduction or re-oxidization of SH groups in the peptide. We excluded the possibility of glycosylation of the

murine Insl6 (Fig. 9A, B &D) as being a reason for the doublet or the discrepancy in size. In addition to post-translational modifications and incomplete reduction of disulfide bonds, excess positive or negative charged residues can result in aberrant mobility of a protein on SDS-PAGE (23, 24). A Glu-rich region (EEEEE) is present (aa 22-26) in the mouse Insl6 peptide. Glu-rich region have been shown to interfere with protein mobility on SDS-PAGE resulting in an artifactual increase in estimation of molecular weight on SDS-PAGE (25) and it is possible that such a phenomenon may be contributing to the slower than predicted mobility of the mouse Insl6 protein on SDS-PAGE. Total amino acids for the myc-his tagged human Insl6 is 249 amino acids and the size of the human prepro- and pro-Insl6 is predicted to be approximately 28 kD and 25 kD respectively. Our results indicate that the size of the human prepro/pro-Insl6 is approximately 35kD before deglycosylation and 32 Kd following deglycosylation. Hence the size of the human Insl6 is approximately 11% larger than the predicted size. We hypothesize that similar to the mouse protein, this discrepancy in molecular size could be due to excess negative charge of tandem glutamic acid residues located at aa 56-58 and aa 102 -103.

The mammalian prohormone convertase (PC) cadre of proteins include furin/PACE, PC1/PC3, PC2, PC4, PACE4, PC5/PC6, PC7/PC8/LPC, SKI/S1P, and NARC-1/PCSK9. CHO cell have been demonstrated to express furin and PC7 and SKI-1 (26-28), and LoVo cells are deficient in furin but express other PC's such as PC7 and PACE4 (29, 30). Our results with the furin inhibitor Dec-RVKR-CMK and furin deficient LoVo cells establish that Insl6 is a target for furin action and that furin is one of the PC's responsible for the 6/8 kDa doublet configuration of the mature protein on gel-electrophoresis. Our results also establish the identity of one of the cleavage sites (RKRR, amino acids 162-165) of the mInsl6 peptide.

Experiments using ectopic expression of furin indicate that this site is a target for furin action. Furthermore, differences in the size of the secreted protein following inhibition of furin activity or mutation of this cleavage site predicts that this site must also be a site for action by non-furin PC(s). It is noteworthy that the molecular weight profiles of proteins synthesized via ectopic expression of Insl6 in GC2 cells were similar to that observed with ectopic expression in CHO cells, suggesting similarity in the Insl6-directed PC activity in these two cell types. The demonstration of the secretory status of Insl6 could provide clues to the cellular targets of Insl6 action. Thus in addition to possible autocrine actions on the germ cell, the physical proximity of the germ cell to the Sertoli cell renders the Sertoli cell a likely candidate for Insl6 action. In this regard the demonstration of Insl6 expression in the brain (31) suggests biological actions of Insl6 outside the testis.

Our studies indicate that Insl6 undergoes other post-translational modifications such as ubiquitination and N-glycosylation in a species-specific manner. Our results establish that the human Insl6 precursor is N-glycosylated, consistent with the *in silico* prediction. In contrast, despite the presence of a computer-predicted putative N-glycosylation site in the mouse Insl6 gene we were unable to demonstrate N-Glycosylation of the murine Insl6 protein in either CHO or GC2 cells and in mouse testis extracts. The functional significance of this differential species-specific glycosylation status of the Insl6 protein remains to be elucidated. Protein ubiquitination is an important form of covalent modification that regulates various cellular processes including cell division, growth, communication/signaling, movement and death/apoptosis (32). The ubiquitin system in the testis plays a role in sperm cell differentiation and the control of cell cycle during spermatogenesis, and mutations in components of the ubiquitin system result in male infertility (33). The ubiquitin proteolytic

system has generally been regarded as a cytosolic or nuclear pathway. However, recent studies have identified the presence of ubiquitin and ubiquitin-activating enzyme associated with a post-ER/pre-Golgi compartment with the intracellular degradation of certain secreted proteins (e.g. preproparathyroid hormone-related protein) being dependent on ubiquination. It is further postulated that ubiquination plays a role in ER quality-control of misfolded molecules during the synthesis of these proteins (19, 34). A single protein can be modified on one or more lysines with a limited number (< 4) ubiquitin molecules (monobiquination) or with lysine-linked chains of ubiquitin (polyubiquination) (35, 36). Whereas, polyubiquinated proteins are targeted for degradation via the proteasome, monoubiquinated proteins are preferentially degraded in the lysosome. With respect to Insl6, inhibition of either the proteasomal pathway or lysosomal enzymatic activity resulted in prolongation of the half-life of the protein, although the effect of lysosomal inhibition was more dramatic and complete. How can the half-life of the Insl6 protein be apparently affected by perturbation of both the proteasome and the lysosomal pathways? We propose that Insl6 is monoubiquinated and that the primary mode of degradation is by the lysosomal pathway. We hypothesize that the partial effect of proteasome inhibitors on Insl6 degradation is the indirect result of lower cellular levels of ubiquitin that can be induced by proteasome inhibitors (37, 38) and does not reflect a direct role of the proteasome in Insl6 degradation. A caveat in our results is that our results regarding ubiquination of Insl6 were obtained exclusively using an *in vitro* system. Further studies will be required to confirm the presence, characteristics, and biological role of *in vivo* ubiquination of the Insl6 protein.

In conclusion, our results indicate that Insl6 is expressed in the germ cells of the testis. Data presented in the current study demonstrate that Insl6 is a disulfide-linked secreted

protein utilizing the classic secretion pathway that undergoes processing from preprohormone to mature hormone with furin playing a role in this processing. Insl6 is also subjected to ubiquitination and N-glycosylation in a species-specific manner.

Acknowledgements

Supported by grants from the NIH (HD HD044436, DK49845 [RKM] and T32DK07729) and the Children's Hospital of Pittsburgh (Renzeihausen Fund), and the Vira I. Heinz Foundation. This work was also supported in part by the Michigan Diabetes Research and Training Center Grant (P60DK-20572) from NIDDK. The authors acknowledge Drs. Serge Nef and Luis F. Parada (University of Texas, Southwestern Medical Center, Dallas) for their generous gift of murine fetal testes RNA, Alnawaz Rehemtulla (University of Michigan) for plasmid expressing furin, and the assistance of Dr. Simon C. Watkins, Director, Center for Biologic Imaging and the Cell Image Core, Center for Reproductive Physiology, University of Pittsburgh.

References

1. **LeRoith D, Shiloach J, Roth J, Lesniak MA** 1980 Evolutionary origins of vertebrate hormones: substances similar to mammalian insulins are native to unicellular eukaryotes. Proc Natl Acad Sci USA 77:6184-6188
2. **Konopinska D, Rosinski G, Sobotka W** 1992 Insect peptide hormones, an overview of the present literature. Int J Pept Protein Res 39:1-11
3. **Smit AB, van Marle A, van Elk R, Bogerd J, vanHeerikhuizen H, Geraerts WP** 1993 Evolutionary conservation of the insulin gene structure in invertebrates: cloning of the gene encoding molluscan insulin-related peptide III from Lymnaea stagnalis. J Mol Endocrinol 11:103-113
4. **Ishizaki H, Suzuki A** 1994 The brain secretory peptides that control moulting and metamorphosis of the silkmoth, Bombyx mori. Int J Dev Bil 38:310
5. **Duret L, Guex N, Peitsch MD, Bairoch A** 1998 New insulin-like proteins with atypical disulfide bond pattern characterized in Caenorhabditis elegans by comparative sequence analysis and homology modeling. Genome Res 8:348-353
6. **Reinecke M, Eppler E, David I, Georges D** 1999 Immunohistochemical evidence for the presence, localization and partial coexistence of insulin, insulin-like growth factor I and relaxin in the protochordate Ciona intestinalis. Cell Tissue Res 295:331-338
7. **Wilkinson T, Speed T, Tregear G, Bathgate R** 2005 Evolution of the relaxin-like peptide family. BMC Evolutionary Biology 5:14
8. **Burkhardt E, Adham IM, Brosig B, Gastmann A, Mattei MG, Engel W** 1994 Structural organization of the porcine and human genes coding for a Leydig cell-specific insulin-like peptide (LEY I-L) and chromosomal localization of the human gene (INSL3). Genomics 20:13-19
9. **Zimmermann S, Steding G, Emmen JM, Brinkmann AO, Nayernia K, Holstein AF, Engel W, Adham IM** 1999 Targeted disruption of the Insl3 gene causes bilateral cryptorchidism. Mol Endocrinol 13:681-691
10. **Chassin D, Laurent A, Janneau JL, Berger R, Bellet D** 1995 Cloning of a new member of the Insulin gene superfamily (INSL4) expressed in human placenta. Genomics 29:465-470
11. **Koman A, Cazaubon S, Couraud PO, Ullrich A, Strosberg AD** 1996 Molecular characterization and in vitro biological activity of placentin, a new member of the insulin gene family. J Biol Chem 271:20238-20241
12. **Conklin D, Lofton-Day CE, Haldeman BA, Ching A, Whitmore TE, Lok S, Jaspers S** 1998 Identification of INSL5, a new member of the insulin superfamily. Genomics 60:50-56
13. **Hsu SY** 1999 Cloning of two novel mammalian paralogs of relaxin/insulin family proteins and their expression in testis and kidney. Mol Endocrinol 13:2163-2174
14. **Kasik J, Muglia L, Stephan DA, Menon RK** 2000 Identification, chromosomal mapping, and partial characterization of mouse Insl6: a new member of the insulin family. Endocrinology 141:458-461
15. **Lok S, Johnston DS, Conklin D, Lofton-Day CE, Adams RL, Jelmberg AC, Whitmore TE, Schrader S, Griswold MD, Jaspers SR** 2000 Identification of INSL6, a new member of the insulin family that is expressed in the testis of the human and rat. Biol Reprod 62:1593-1599

16. **Liu C, Eriste E, Sutton S, Chen J, Roland B, Kuei C, Farmer N, Jornvall H, Sillard R, Lovenberg TW** 2003 Identification of Relaxin-3/INSL7 as an Endogenous Ligand for the Orphan G-protein-coupled Receptor GPCR135. J Biol Chem 278:50754-50764
17. **Hardy S, Kitamura M, Harris-Stansil T, Dai Y, Phipps ML** 1997 Construction of adenovirus vectors through Cre-lox recombination. J Virol 71:1842-1849
18. **Yu JH, Schwartzbauer G, Kazlman A, Menon RK** 1999 Role of the Sp family of transcription factors in the ontogeny of growth hormone receptor gene expression. J Biol Chem 274:34327-34336
19. **Meerovitch K, Wing S, Goltzman D** 1997 Preproparathyroid Hormone-related Protein, a Secreted Peptide, Is a Substrate for the Ubiquitin Proteolytic System. J Biol Chem 272:6706-6713
20. **Chomczynski P, Sacchi N** 1987 Single-step method of RNA isolation by acid guanidinium thiocyanate-phenol-chloroform extraction. Anal Biochem 162:156-159
21. **Gibson UE, Heid CA, Williams PM** 1996 A novel method for real time quantitative RT-PCR. Genome Res 6:995-1001
22. **Biosystems PA** 1997 ABI Prism 7700 Sequence Detection System, Relative Quantitation of Gene Expression. PE Applied Biosystems User Bulletin 2
23. **Hu CC, Ghabrial SA** 1995 The conserved, hydrophilic and arginine-rich N-terminal domain of cucumovirus coat proteins contributes to their anomalous electrophoretic mobilities in sodium dodecylsulfate-polyacrylamide gels. J Virol Methods 55:367-379
24. **Armstrong DJ, Roman A** 1993 The anomalous electrophoretic behavior of the human papillomavirus type 16 E7 protein is due to the high content of acidic amino acid residues. Biochem Biophys Res Commun 192:1380-1387
25. **Iakoucheva LM, Kimzey AL, Masselon CD, Smith RD, Dunker AK, Ackerman EJ** 2001 Aberrant mobility phenomena of the DNA repair protein XPA. Protein Sci 10:1353-1362
26. **Nour N, Basak A, Chretien M, Seidah NG** 2003 Structure-function analysis of the prosegment of the proprotein convertase PC5A. J Biol Chem 278:2886-2895
27. **Gu M, Rappaport J, Leppla SH** 1995 Furin is important but not essential for the proteolytic maturation of gp160 of HIV-1. FEBS Lett 365:95-97
28. **Pullikotil P, Vincent M, Nichol ST, Seidah NG** 2004 Development of protein-based inhibitors of the proprotein of convertase SKI-1/S1P: processing of SREBP-2, ATF6, and a viral glycoprotein. J Biol Chem 279:17338-17347
29. **Takahashi S, Nakagawa T, Kasai K, Banno T, Duguay SJ, Van de Ven WJ, Murakami K, Nakayama K** 1995 A second mutant allele of furin in the processing-incompetent cell line, LoVo. Evidence for involvement of the homo B domain in autocatalytic activation. J Biol Chem 270:26565-26569
30. **Seidah NG, Hamelin J, Mamarbachi M, Dong W, Tardos H, Mbikay M, Chretien M, Day R** 1996 cDNA structure, tissue distribution, and chromosomal localization of rat PC7, a novel mammalian proprotein convertase closest to yeast kexin-like proteinases. Proc Natl Acad Sci U S A 93:3388-3393
31. **Brailoiu GC, Dun SL, Yin D, Yang J, Chang JK, Dun NJ** 2005 Insulin-like 6 immunoreactivity in the mouse brain and testis. Brain Research 1040:187-190
32. **Hershko A, Ciechanover A** 1998 The ubiquitin system. Annu Rev Biochem 67:425-479

33. **Sutovsky P** 2003 Ubiquitin-dependent proteolysis in mammalian spermatogenesis, fertilization, and sperm quality control: Killing three birds with one stone. Microsc Res Tech 61:88-102
34. **Yeung S, Chen S, Chan L** 1996 Ubiquitin-proteasome pathway mediates intracellular degradation of apolipoprotein B. Biochemistry 35:13843–13848
35. **Hicke L** 2001 Protein regulation by monoubiquitin. Nat Rev Mol Cell Biol 2:195-201
36. **Weissman AM** 2001 Themes and variations on ubiquitylation. Nat Rev Mol Cell Biol 2:169-178
37. **Schubert U, Ott DE, Chertova EN, Welker R, Tessmer U, Princiotta MF, Bennink JR, Krausslich HG, Yewdell JW** 2000 Proteasome inhibition interferes with gag polyprotein processing, release, and maturation of HIV-1 and HIV-2. Proc Natl Acad Sci U S A 97:13057-13062
38. **Mimnaugh EG, Chen HY, Davie JR, Celis JE, Neckers L** 1997 Rapid deubiquitination of nucleosomal histones in human tumor cells caused by proteasome inhibitors and stress response inducers: effects on replication, transcription, translation, and the cellular stress response. Biochemistry 36:14418-14429

Figure Legends

Fig. 1 - Immunohistochemical detection of Insl6 expression in germ cells of the testis. Insl6 expression in testicular section from mice (8 wk old) using anti-Insl6 antibody (EE) without (A,C) and with (B,D) presaturation with antigen peptide (x200). The binding of the primary antibody was either visualized by light microscopy using the avidin-biotin HRP methodology (A,B) or via confocal microscopy of sections labeled with Cy-3 conjugated secondary antibody (C,D). The slides were also counterstained with either hemotoxylin (A,B) or Sytox green (C,D). The specific staining of leptotene spermatocytes (L), pachytene spermatocytes (P), spermatids (S), and elongated spermatids (ES) are indicated by solid arrows. The results are representative of two or more independent experiments. Scale bar = 25 µm in A&B; Scale Bar = 10 µm in C&D.

Fig. 2 - Effect of germ cell aplasia on Insl6 mRNA and protein expression. Panels A & B - Steady state abundance of Insl6 mRNA was measured by real-time quantitative RT-PCR assay in testis of rats (Panel A) or mice (Panel B) (n =3-7). The abundance of LH receptor mRNA was assayed as a marker of germ cells. Panel A - Rats exposed to radiation during fetal life compared with non-exposed control rats; Panel B - Germ cell aplasia mice WBB6F1/J-Kit^{W}/Kit^{W-v} compared with the control mice, WB/ReJ Kit^{w}/+. The values are represented relative to level of expression in the vehicle treated group and are depicted as mean and range. The range is determined by evaluating the expression $2^{-\Delta\Delta}C_T$ with $^{\Delta\Delta}C_T + s$ and $^{\Delta\Delta}C_T - s$, where s is the standard deviation (SD) of the $^{\Delta\Delta}C_T$ value (PE Applied Biosystems, 1997). * = $p<0.01$ compared to the control group by ANOVA.

Fig. 3 - Insl6 expression: ontogeny and tissue distribution. Panel A - Ontogeny of Insl6 expression in mouse testis. Expression of Insl6 mRNA was measured by real-time quantitative RT-PCR assay in testis of mice (n =3-5) at indicated ages. The values (mean ± SE) are represented as relative to level of Insl6 mRNA at 90 days designated as 100%. e = embyronic, p = postnatal. **Panel B -** Tissue specific expression of Insl6. Insl6 mRNA levels were measured by real-time quantitative RT-PCR assay in the indicated tissues of adult (6-8 wk old; n = 3-5) male (small bowel, kidney, spleen, and thymus) or female (uterus and breast). The levels are depicted as relative to Insl6 abundance in testis designated as 100%. The results are depicted as mean and range. The range is determined by evaluating the expression, $2^{-\Delta\Delta}C_T$ with ${}^{\Delta\Delta}C_T + s$ and ${}^{\Delta\Delta}C_T - s$, where s is the standard deviation (SD) of the ${}^{\Delta\Delta}C_T$ value (PE Applied Biosystems, 1997).

Fig. 4 - Sub-cellular localization of Insl6 by co-immunofluorescence. Panel A - CHO cells stably expressing either c-myc-tagged mInsl6 (i-iii) or hInsl6 (iv-vi) were fixed, permeablized and incubated with primary antibodies, mouse anti-myc, or rabbit anti-Bip. The specific binding of the primary antibodies were detected by using FITC-labeled anti-mouse IgG or Rhodamine-labeled anti-rabbit IgG respectively. Immunofluorescence staining for Insl6 (i & iv) and the ER marker Bip 78 (ii & v) depict identical patterns as illustrated in the merged panels (iii & vi). The results are representative of three or more independent experiments. **Panel B** – GC2 cells exhibiting adenovirus-mediated mInsl6 expression (i, ii & iii) or CHO cells stably expressing c-myc-tagged mInsl6 (iv-ix) were fixed, permeablized and incubated with primary antibodies, rabbit anti-myc, or mouse anti-GM130. The specific binding of the

primary antibodies were detected by using FITC-labeled anti-mouse IgG or Rhodamine-labeled anti-rabbit IgG respectively. Immunofluorescence staining for Insl6 (i & iv) and the Golgi marker GM 130 (ii & v) depict overlapping patterns as illustrated in the merged panels (iii & vi). To further demonstrate the Golgi localization of Insl6, mInsl6-CHO cells were exposed to Nocodazole (vii, viii, & ix) prior to fixation and immunofluorescence staining for Insl6 (vii) and the Golgi marker GM130 (viii) as described above. The disruption of Golgi by Nocodozole and consequent parallel redistribution of GM 130 and Insl6 is illustrated in the merged panel (ix). The results are representative of two independent experiments.

Fig. 5 - Insl6 is a secreted protein. Naïve CHO cells (lane 1), CHO cells stably expressing c-myc-tagged mInsl6 (lane 2), Ad-mInsl6 infected GC2 (lane 3) or naïve GC2 cells (lane 4) were maintained overnight in DMEM medium supplemented with 2% FBS. The cells (top panel) and culture medium (bottom panel) were harvested separately and processed for analysis. Approximately 2% of whole cell lysate (top panel) and 20% of the concentrated culture medium (bottom panel) (from 35mm culture plate) was subjected to SDS-PAGE size fractionation under reducing conditions and Western blot analysis with anti c-myc antibody for the presence of the Insl6 protein. The predicted compositions of the various Insl6 bands and the positions of the molecular weight marker are indicated.

Fig. 6 – Secretion of Insl6 is sensitive to brefeldin A (BFA) treatment. Panel A - CHO cells stably expressing c-myc-tagged mInsl6 were treated with BFA at the indicated concentration for 6 hr and the culture medium (top panel lane 2-7) and cells (top panel lane 1, bottom panel lane1-5) harvested separately and processed for analysis. Approximately 20% of

the culture medium from culture plate (35mm) was subjected to SDS-PAGE size fractionation under reducing conditions and Western blot analysis with anti c-myc antibody for presence of the Insl6 protein. The predicted compositions of the various Insl6 bands and the positions of the molecular weight marker are indicated. **Panel B** – Insl6-adenovirus (Ad-mInsl6) infected GC2 cells were treated with BFA at the indicated concentration for overnight and the culture medium were harvested and processed for analysis. Approximately 20% of the concentrated culture medium (from 35mm culture plate) was subjected to SDS-PAGE size fractionation under reducing conditions and Western blot analysis with anti c-myc antibody for presence of the Insl6 protein. The predicted compositions of the various Insl6 bands and the positions of the molecular weight marker are indicated.

Fig. 7 - Insl6 is a target for processing by furin. Top panel - Processing of Insl6 protein in CHO and furin deficient LoVo cells. Supernatants of CHO cells stably expressing c-myc-tagged mInsl6 (lane 1), CHO cells transiently transfected with furin cleavage site mutant mouse c-myc tagged Insl6 (lane 2), LoVo cells transiently transfected with wild type mouse c-myc tagged Insl6 (lanes 3 and 4) or LoVo cells transiently transfected with furin cleavage site mutant mouse c-myc tagged Insl6 (lanes 5 and 6) in the absence (lanes 3 and 5) or presence (lanes 4 and 6) of ectopic expression of human furin were size-fractioned by SDS-PAGE under reducing conditions and analyzed by Western blot analysis with anti c-myc antibody for presence of the Insl6 protein as described in Materials and Methods. Approximately 20% of the culture medium from each transfection was subjected to this analysis. The predicted compositions of the various Insl6 bands and the positions of the molecular weight marker are indicated. **Bottom panel** - Processing of Insl6 protein in the presence of furin inhibitor Dec-

RVKR-CMK. CHO cells stably expressing c-myc-tagged mInsl6 were cultured in 2% serum and treated with 25 μM of furin inhibitor Dec-RVKR-CMK for 24 hours (lane 3). Control cells were treated with equal amount of solvent (methanol, lane 2) or without methanol (lane 1). Approximately 20% of the culture medium (from 35mm culture plate) was subjected to SDS-PAGE size fractionation and Western blot analysis with anti c-myc antibody for presence of Insl6 protein. The predicted compositions of the various Insl6 bands and the positions of the molecular weight marker are indicated.

Fig. 8 – Presence of disulfide bonds in Insl6. Panel A - Intramolecular disulfide bonds in mouse Insl6**.** Whole cell lysates (top panel) or cell culture supernatant (bottom panel) of CHO cells stably expressing c-myc-tagged mInsl6 protein (mInsl6-CHO; lanes 1-6 top panel and lanes 2-5 bottom panel) or untransfected CHO cells (bottom panel, lanes 1 and 6) were size-fractionated by SDS-PAGE electrophoresis under either non-reducing conditions (top panel: lane 1, non-boiled, lane 2, boiled; bottom panel: lanes 1 and 2 non-boiled) or reducing conditions (DTT, 1-100 mM, lanes 3-6, top and bottom panels). The electrophoretic mobility of the Insl6 protein was analyzed by Western blot analysis using anti c-myc antibody. The predicted compositions of the various Insl6 bands and the positions of the molecular weight marker are indicated. **Panel B –** Differences in disulfide bond formation between mouse and human Insl6 proteins. Cell culture supernatant of CHO cells expressing c-myc-tagged human (lane 1 and 3) or mInsl6 protein (lanes 2 and 4) were size-fractionated by SDS-PAGE electrophoresis under either non-reducing conditions (lane 1 and 2) or reducing conditions (100 mM DTT, lanes 3 and 4). The electrophoretic mobility of the Insl6 protein was analyzed

by Western blot analysis using anti c-myc antibody. The predicted compositions of the various Insl6 bands and the positions of the molecular weight marker are indicated.

Fig. 9 - Differential N-linked glycosylation of murine and human Insl6 proteins. Panel A. *Top panel* **–** Whole cell lysates of CHO cells stably expressing c-myc-tagged human Insl6 protein were exposed to PNGase F enzyme (+) or vehicle (-) and the products size-fractionated by SDS-PAGE electrophoresis under reducing conditions and characterized by western blot analysis using anti c-myc antibody. The positions of the specific bands (1, 1a, 2, and 2a) and the molecular weight markers are indicated. Bands 1a and 2a possibly represent deglycosylated forms of bands 1 and 2 respectively. *Bottom Panel* – Whole cell lysates of CHO cells stably expressing c-myc-tagged mInsl6 protein were exposed to PNGase F enzyme (+) or vehicle (-) and the products size-fractionated by SDS-PAGE electrophoresis under reducing conditions and characterized by Western blot analysis using anti c-myc antibody. The positions of the molecular weight markers are indicated. **Panel B** – Protein extracts of CHO cells or Insl6-adenovirus (Ad-mInsl6) infected GC2 cells were exposed to PNGase F enzyme (+) or vehicle (-) and the products size-fractionated by SDS-PAGE electrophoresis under reducing conditions and characterized by Western blot analysis using anti c-myc antibody. Lane 1-2, naïve CHO cells, lane 3-4 CHO cells stably expressing hInsl6, lane 5-6, GC2 cells expressing adenovirally mediated mInsl6, lane 7-8, naïve GC2. The cell extracts were treated with PNGase F in certain instances (lanes 2, 4, 6, 8). The positions of the molecular weight markers are indicated. The results are representative of three independent experiments. **Panel C -** Whole cell lysates of CHO cells stably expressing c-myc-tagged hInsl6 protein were exposed to endo H enzyme (+) or vehicle (-) and the products size-

fractionated by SDS-PAGE electrophoresis under reducing conditions and characterized by Western blot analysis using anti c-myc antibody. The position of the molecular weight marker is indicated. Panel D – *Top panel* - aliquots of mouse testis or liver whole cell extracts were exposed to PNGase F enzyme (+) or vehicle (-) and the products size-fractionated by SDS-PAGE electrophoresis under reducing conditions and characterized by Western blot analysis using anti-Insl6 antibody (EE). The positions of the molecular weight markers are indicated. *Bottom panel* - - aliquots of whole cell extracts of either mouse germ cells (lane 1) or liver (lane 2) were size-fractionated by SDS-PAGE electrophoresis under reducing conditions and characterized by Western blot analysis using anti-Insl6 A peptide antibody (Phoenix Pharmaceuticals, Inc). The position of the molecular weight marker is indicated.

Fig. 10 - Insl6 is an ubiquinated protein. Panel A – *In vitro* ubiquination of mouse Insl6. Coupled *in vitro* transcription-translation reaction using wheat germ extract (lane 1) or reticulocyte lysate (lanes 2 and 3) was used to synthesize [^{35}S] cysteine-labeled mInsl6 in the absence (-) or presence (+) of His tagged ubiquitin. The products were size fractionated via SDS-PAGE electrophoresis and visualized by autoradiograhy. The position of putatively ubiquinated higher molecular weight products are indicated in both the reaction without (◀) and with (←) His-ubiquitin. Note the apparent increase in molecular weight of the bands in the His-ubiquitin reactions. **Panel B -** Degradation of mInsl6 *in vitro* is ATP dependent. mInsl6 protein was expressed in a transcription-translation coupled system where either ATP (+) or ATP-depleting mixture (-) was added 30 minutes after initiation of the reaction. Aliquots of the reaction at the indicated time-periods were analyzed by SDS-PAGE and autoradiography. **Panel C -** Degradation of Insl6 is blocked by proteasome inhibitors *in vivo*.

CHO cells stably expressing c-myc tagged mInsl6 were either exposed to vehicle (-) or 5 μM Clasto-Lactacystin-β-lactone (CL) (+) and cells harvested after 4 h (lanes 1 & 2) or 24 h (lanes 3 & 4). The cell lysates were analyzed by Western blot using anti-myc antibody. **Panel D -** Degradation of Insl6 is blocked by proteasome inhibitors *in vitro.* Coupled *in vitro* transcription / translation of Insl6 using reticulocyte lysates performed for the indicated time (hrs) in the presence of either vehicle (-) or 5 μM Clasto-Lactacystin-β-lactone (Clasto-L) (+). The reaction products were size-fractionated via SDS-PAGE and autoradiographed**. Panel E -** Stability of Insl6 in the presence of proteasomal or lysosomal inhibitor. CHO cells stably expressing c-myc tagged mInsl6 were exposed to vehicle, proteasomal inhibitor (Clasto-Lactocysteine [CL], 10μM), lysosomal inhibitors (chloroquine [CQ] 0.2mM or bafilomycin [Baf] 1 μM). mInsl6 protein expressed in these cells was pulse labeled using [^{35}S] cysteine and chased with unlabelled cysteine. At the indicated time points, cells were harvested, immunoprecipitated with anti-myc (9E10) monoclonal antibody, and analyzed by SDS-PAGE as described in Materials and Methods. For a graphical representation of the results the intensity of the specific bands was quantified by densitometry and the results depicted as relative to intensity of the band at time "0" designated as 100%. The X-axis is depicted in log and the Y-axis in linear scale.

Fig. 11 - Mouse Insl6 protein. The predicted signal peptide (italicized), B chain (boxed), C chain (in grey), and A chain (boxed) are specified. The putative locations of the disulfide bonds and furin cleavage site are indicated.

Table 1: Sequence of Primer-Probe Sets used in the Real-Time RT-PCR Assay

	Primer/probe	**Sequence**
Mouse Insl6	Forward	TCACGCAAGGGCAAAGC
	Reverse	GGGACTGGGTTTGTGAATCTTC
	Probe (FAM)	AACCCTCACCCTTCTTCCTCCGCCT
Rat Insl6	Forward	CCCAACTATCAGCTTAAAAAGGA
	Reverse	CGCTGAAGGTACTCATTTTGTCA
	Probe (FAM)	CATTCATACCACGGTGGCAAGCCC
Rat LHR	Forward	ACATTGAACCTGGTGCTTTTACAA
	Reverse	AGGGTTCGGATGCCTGTG
	Probe (FAM)	CCTCCCTCGGTTAAAATACCTGAG CATCTGTA
18S	Primers	Proprietary (Applied Biosystems)
	Probe(VIC)	Proprietary (Applied Biosystems)

5'-end reporter dyes: FAM [6-carboxy-fluorescein] and VIC (proprietary; PE Biosystems). The quencher fluorescent dye at the 3'-end was TAMRA [6-carboxy-tetramethyl-rhodamine) for all probes.

Fig. 1

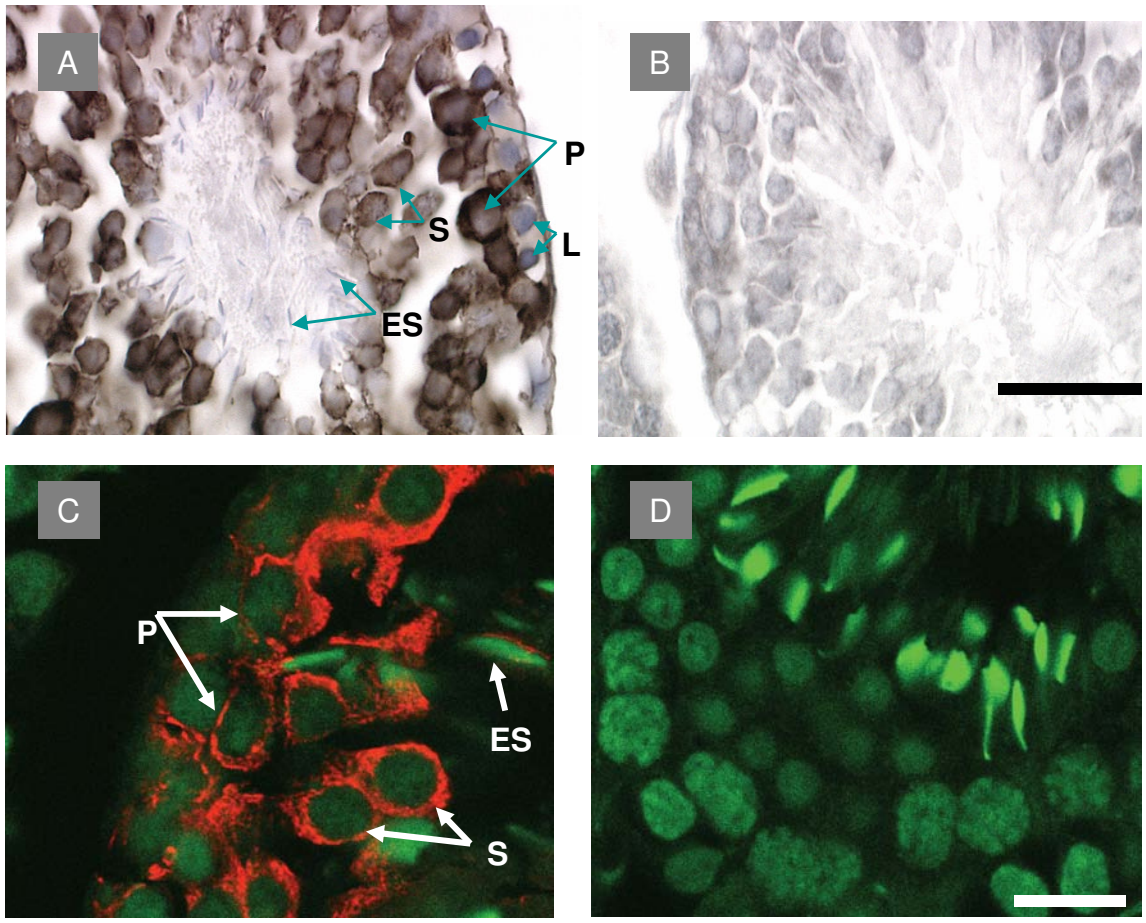

Fig. 2

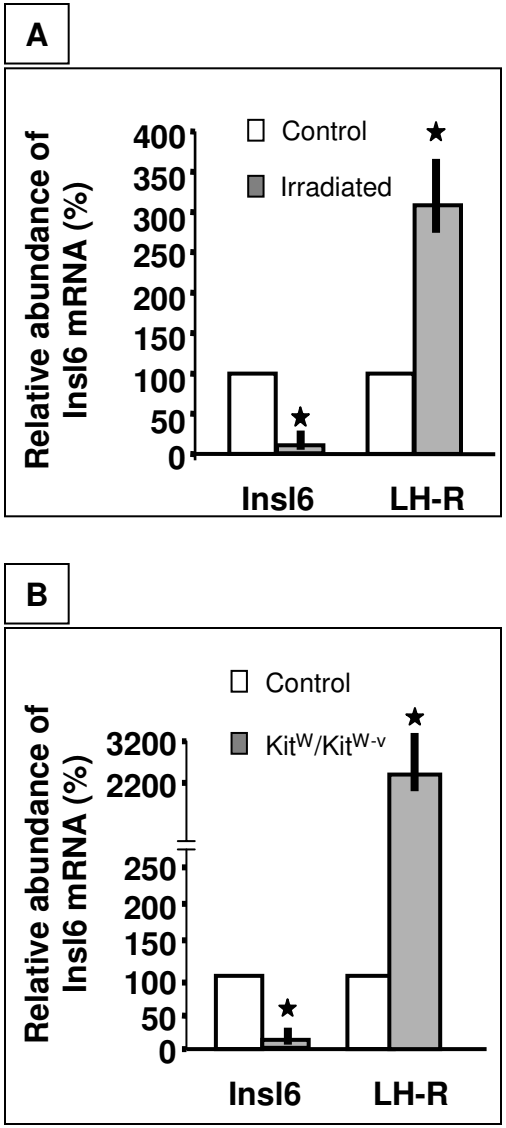
A
Relative abundance of Insl6 mRNA (%)
400
350
300
250
200
150
100
50
0
Control
Irradiated
Insl6
LH-R
B
Relative abundance of Insl6 mRNA (%)
3200
2200
250
200
150
100
50
0
Control
Kit^W/Kit^W-v
Insl6
LH-R

Fig. 3

A

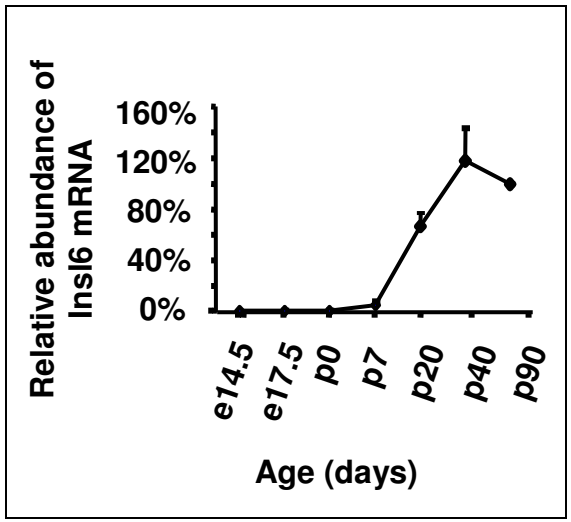
Relative abundance of Insl6 mRNA
160%
120%
80%
40%
0%
e14.5
e17.5
p0
p7
p20
p40
p90
Age (days)

B

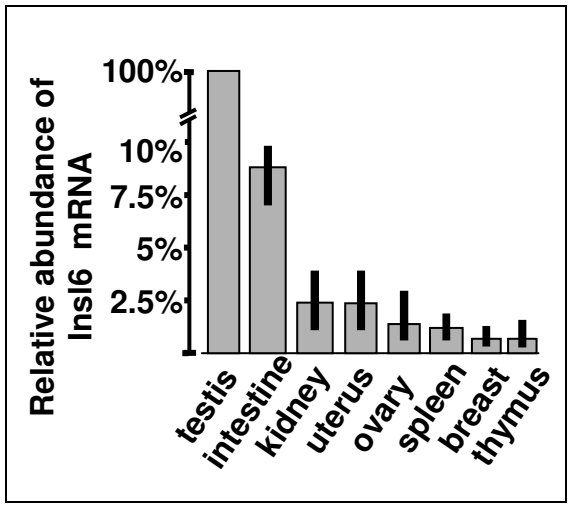
Relative abundance of Insl6 mRNA
100%
10%
7.5%
5%
2.5%
testis
intestine
kidney
uterus
ovary
spleen
breast
thymus

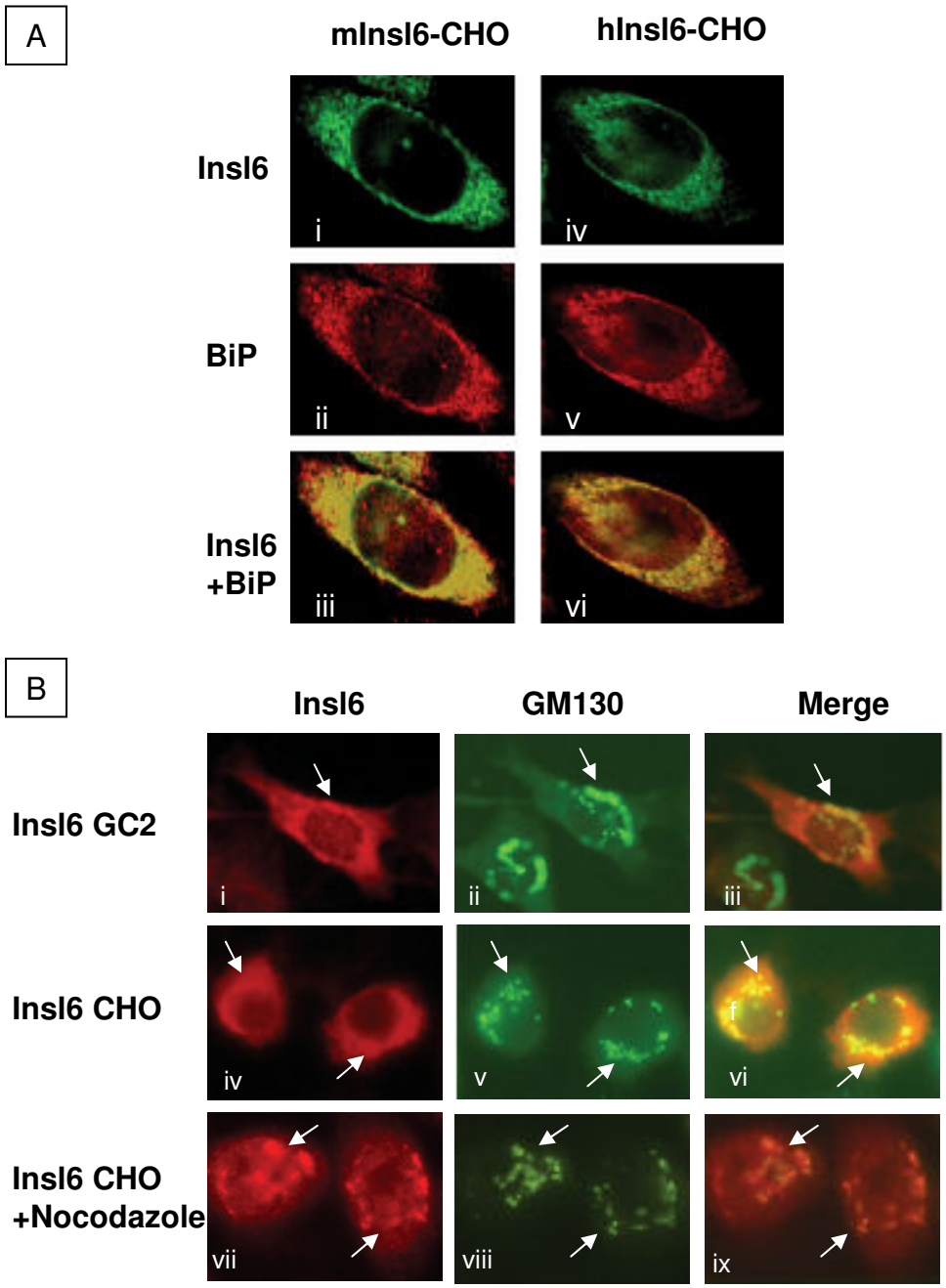
A
mInsl6-CHO
hInsl6-CHO
Insl6
BiP
Insl6
+BiP
i
ii
iii
iv
v
vi
B
Insl6
GM130
Merge
Insl6 GC2
Insl6 CHO
Insl6 CHO
+Nocodazole
i
ii
iii
iv
v
vi
vii
viii
ix

Fig. 5

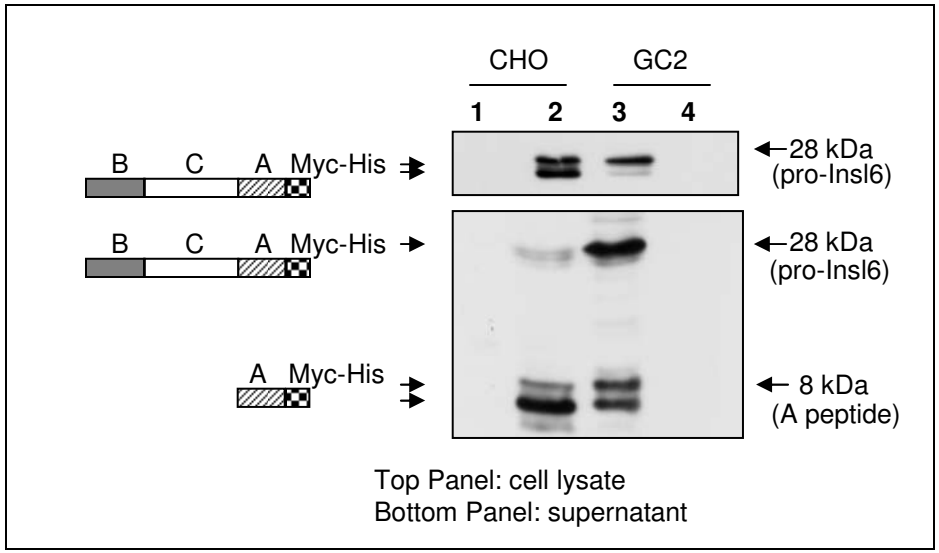
CHO
GC2
1
2
3
4
B C A Myc-His
B C A Myc-His
A Myc-His
28 kDa
(pro-Insl6)
28 kDa
(pro-Insl6)
8 kDa
(A peptide)
Top Panel: cell lysate
Bottom Panel: supernatant

Fig. 6

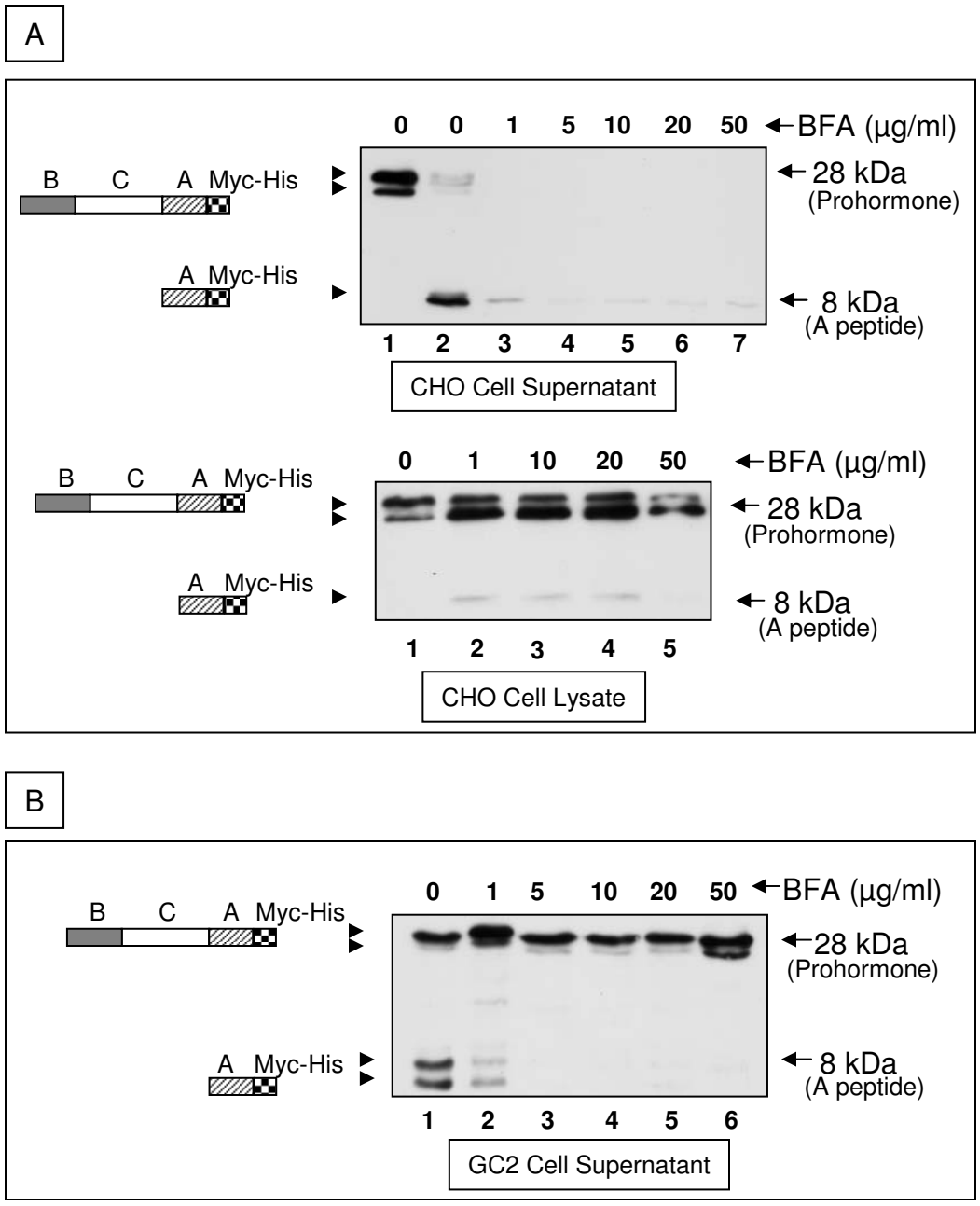
A
0 0 1 5 10 20 50 ←BFA (μg/ml)
B C A Myc-His
A Myc-His
←28 kDa
(Prohormone)
← 8 kDa
(A peptide)
1 2 3 4 5 6 7
CHO Cell Supernatant
0 1 10 20 50 ←BFA (μg/ml)
B C A Myc-His
A Myc-His
←28 kDa
(Prohormone)
← 8 kDa
(A peptide)
1 2 3 4 5
CHO Cell Lysate
B
0 1 5 10 20 50 ←BFA (μg/ml)
B C A Myc-His
A Myc-His
←28 kDa
(Prohormone)
← 8 kDa
(A peptide)
1 2 3 4 5 6
GC2 Cell Supernatant

Fig. 7

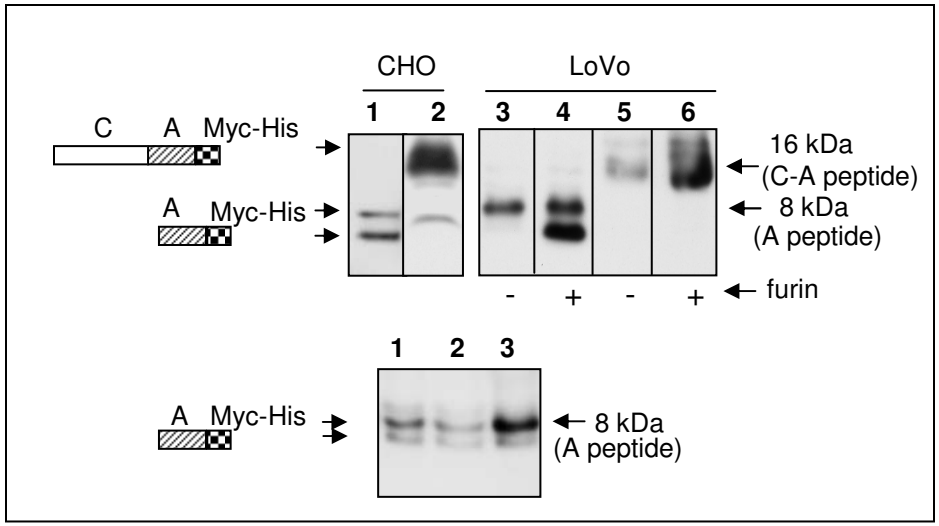
CHO
LoVo
1 2 3 4 5 6
C A Myc-His
A Myc-His
16 kDa
(C-A peptide)
8 kDa
(A peptide)
- + - +
furin
1 2 3
A Myc-His
8 kDa
(A peptide)

Fig. 8

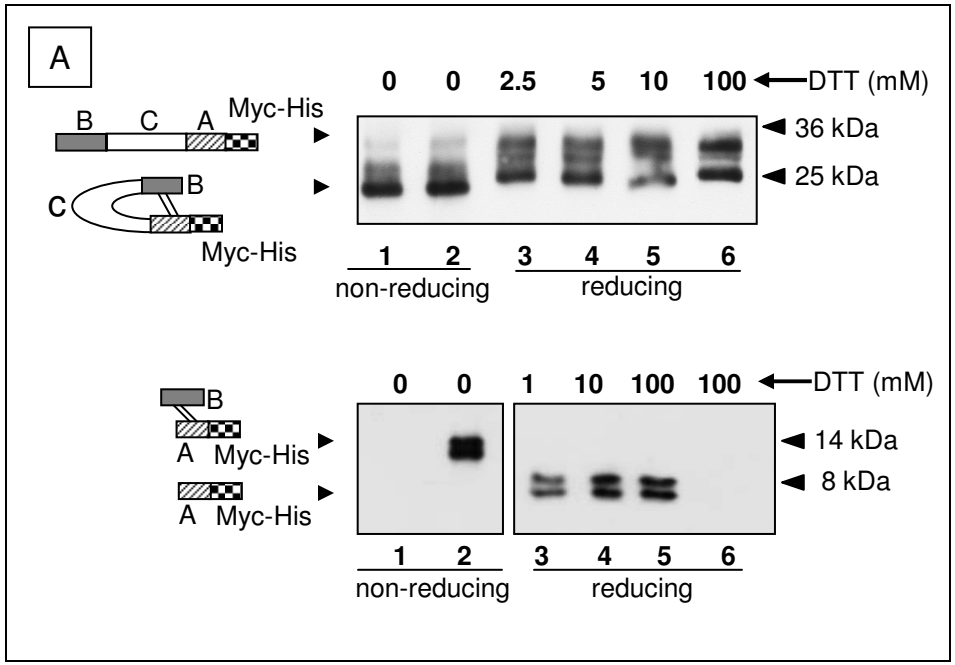
A
B C A Myc-His
C B Myc-His
0 0 2.5 5 10 100 DTT (mM)
36 kDa
25 kDa
1 2 3 4 5 6
non-reducing
reducing
B A Myc-His
A Myc-His
0 0 1 10 100 100 DTT (mM)
14 kDa
8 kDa
1 2 3 4 5 6
non-reducing
reducing

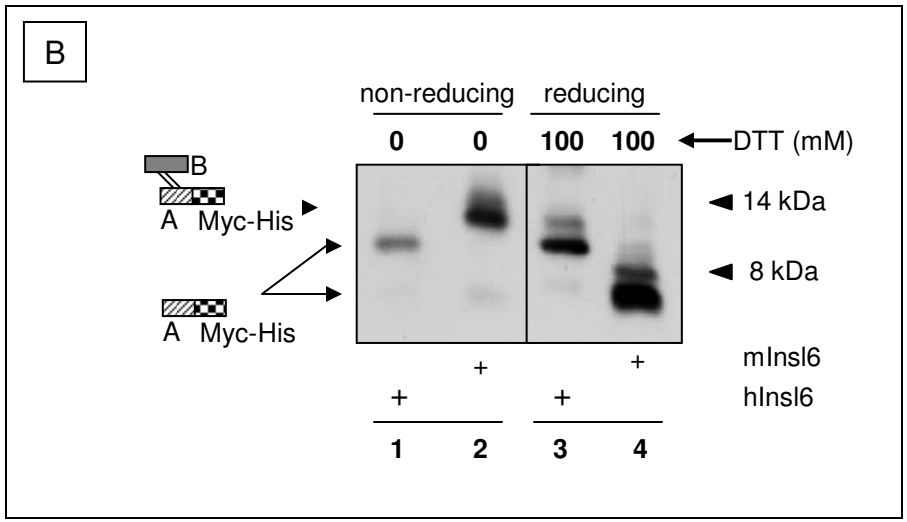
B
non-reducing
reducing
0 0 100 100 DTT (mM)
B A Myc-His
A Myc-His
14 kDa
8 kDa
mInsl6
hInsl6
+ + + +
1 2 3 4

Fig. 9

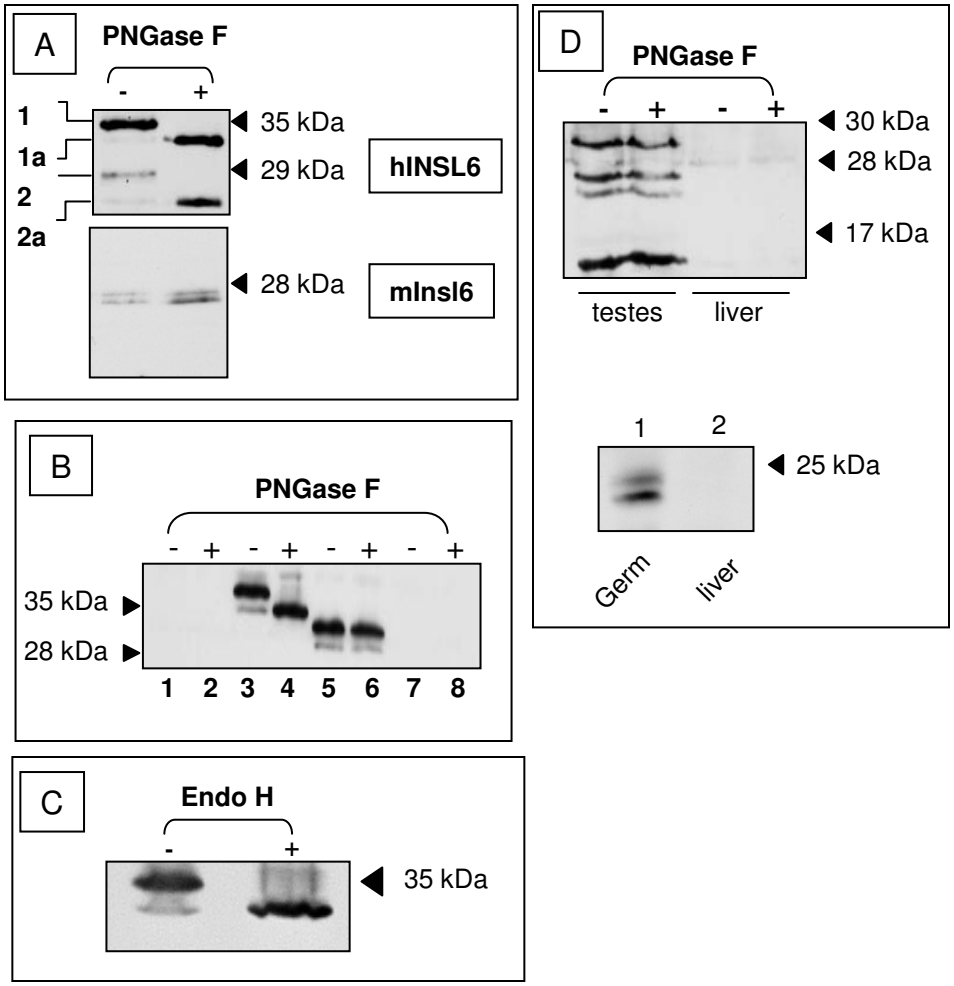
A
PNGase F
-
+
1
1a
2
2a
35 kDa
29 kDa
hINSL6
28 kDa
mInsl6
B
PNGase F
- + - + - + - +
35 kDa
28 kDa
1 2 3 4 5 6 7 8
C
Endo H
-
+
35 kDa
D
PNGase F
- + - +
30 kDa
28 kDa
17 kDa
testes
liver
1 2
25 kDa
Germ
liver

Fig. 10

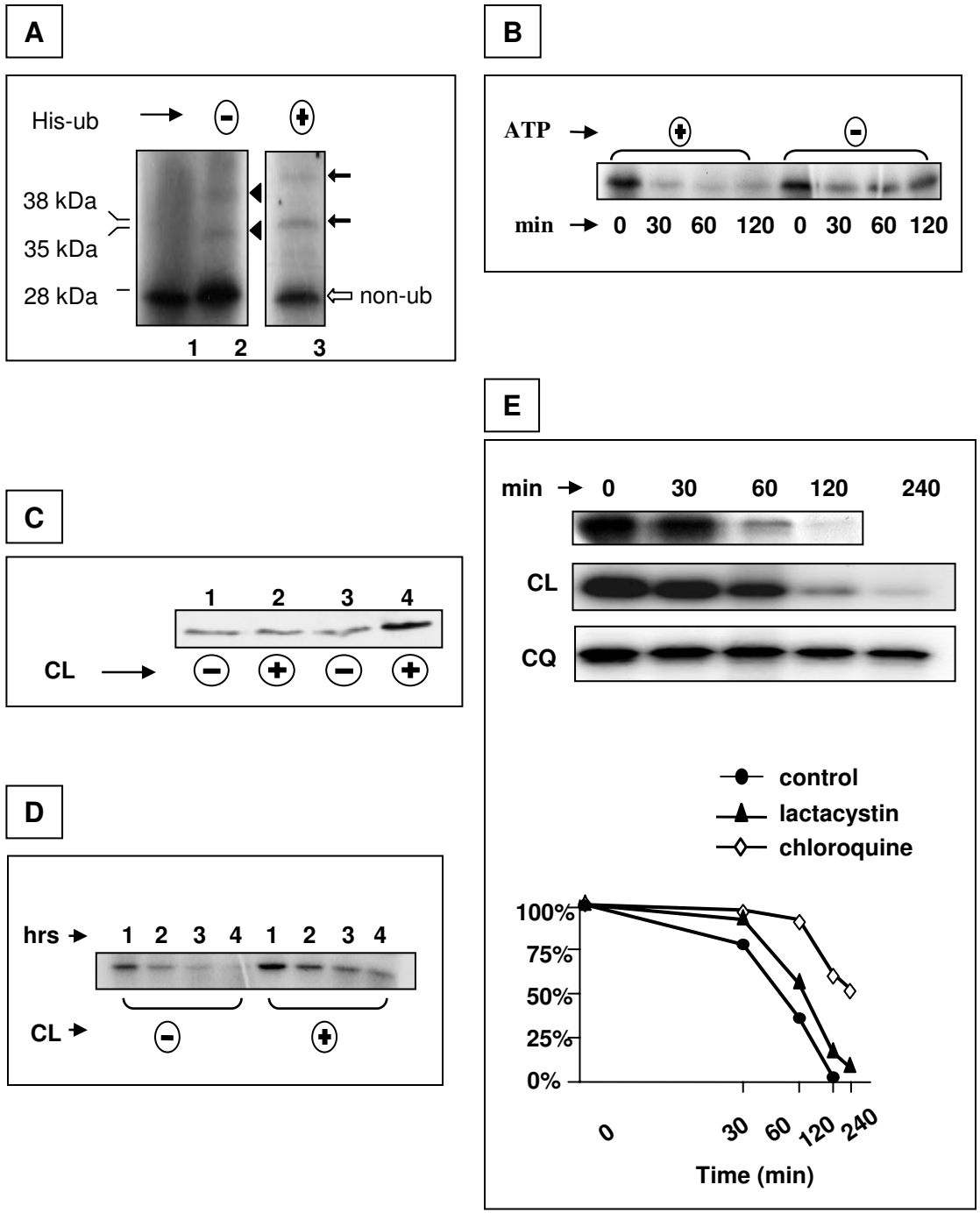
A
His-ub
38 kDa
35 kDa
28 kDa
non-ub
1 2 3
B
ATP
min
0 30 60 120 0 30 60 120
C
1 2 3 4
CL
D
hrs
1 2 3 4 1 2 3 4
CL
E
min
0 30 60 120 240
CL
CQ
control
lactacystin
chloroquine
100%
75%
50%
25%
0%
0 30 60 120 240
Time (min)

Fig. 11

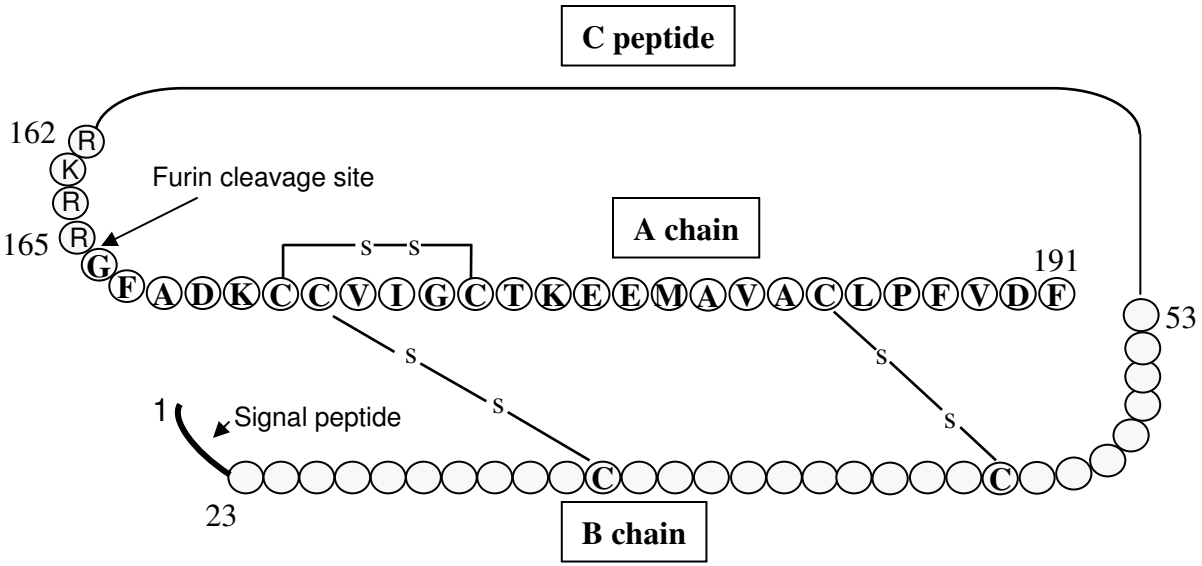

***MKQLCCSCLLWLGLLLTPFSRE*EEEESRPRKLCGRHL**
LIEVIKLCGQSDWSRFEMEEQSPMTQFFPHYSRKGK
AFNPHPSSSAWRRFTNPVPAGVSQKKGTHTWEPQS
LPDYQFEKTELLPKARVFSYHSGKPYVKSVQLQKKS
TNKMNTFRSLFWGNHSQRKRR**GFADKCCVIGCTKE**
EMAVACLPFVDF